EFDA–JET–PR(10)06

J.A. Romero and JET EFDA contributors

Tokamak Internal Inductance Dynamics

Tokamak Internal Inductance Dynamics

J.A. Romero and JET EFDA contributors*

JET-EFDA, Culham Science Centre, OX14 3DB, Abingdon, UK

[1]Asociación EURATOM-CIEMAT, Avenida Complutense 22, E-28040 Madrid, Spain
** See annex of F. Romanelli et al, "Overview of JET Results",*
(Proc. 22 nd IAEA Fusion Energy Conference, Geneva, Switzerland (2008)).

Preprint of Paper to be submitted for publication in
Nuclear Fusion

ABSTRACT

A lumped parameter model for tokamak plasma current and inductance time evolution as function of plasma resistance, non-inductive current drive sources and boundary voltage or Poloidal Field (PF) coil current drive is presented. Having in mind its application in a tokamak inductive control system, the model is expressed in state space form, the preferred choice for the design of control systems using modern control systems theory. The choice of system states allow many interesting physical quantities such as plasma current, inductance, magnetic energy, resistive and inductive fluxes etc be made available as output equations.

The model is derived from energy conservation and flux balance theorems, together with a first order approximation for flux diffusion dynamics. The validity of this approximation has been checked using experimental data from JET showing an excellent agreement.

1. INTRODUCTION

Tokamaks are pulsed devices modelled as a toroidal transformer with one turn secondary R,L plasma ring circuit coupled with a primary transformer circuit.

The inductance of a conventional electrical system is a parameter depending solely on geometrical factors, but at high frequencies non geometrical effects arise as a result of the slow flux penetration inside the conductor, or skin effect [1],[2] . These are taken into account by decomposing the inductance into a geometry dependent part, the external inductance, and a frequency dependent part, the internal inductance. External and internal contributions also account for energy stored in the magnetic field outside and inside the conductor.

Due to the small size of conventional circuits conductors, the skin effect in conventional circuits starts to be taken into consideration at relatively high frequencies.

The time for flux penetration in tokamaks, however, ranges from a fraction of a second to several seconds, due to the large machine size (several meters) and high temperature (several keV). A further difference is that inductance in conventional circuits is analysed in the context of AC excitation and frequency response, while Tokamaks are operated in just half a cycle, and state space time domain model is more appropriate for the analysis.

In a Tokamak, an internal inductance accounts for the energy stored in the poloidal field created by the plasma current and external poloidal field currents, while a mutual inductance accounts for the flux linkage between primary inductive coils and the secondary, which is the plasma ring itself. An equivalent ohmic resistance accounts for the Joule losses in the plasma

[3],[4] .The internal inductance in a tokamak evolves as the magnetic flux and associated internal current density distribution diffuses in the plasma, and also as the external equilibrium field imposed by external poloidal field coils evolves to maintain the plasma within the vacuum vessel boundaries.

Control of internal inductance at a low value is required to extend the duration of tokamak plasma discharges with a limited amount of flux in the transformer primary circuit [5] , [6], to reduce the growth rate of the vertical instability of elongated plasmas [7],[8], and to guarantee access to advanced tokamak scenarios with limited amount of flux available at the transformer primary circuit [9]. Tokamak Inductive control has also been shown to be able to shape q profiles and maintain internal transport barriers [10].

The development of these control systems starts by obtaining a lumped parameter models that approximate processes best described by distributed parameter simulations [11]. To be able to use modern control theory, these models must describe the time evolution of the controlled variables as function of the available actuator and disturbance inputs using the state space formalism. Having in mind its application in a tokamak inductive control system, this work develops such a lumped parameter state space model describing the dynamics of plasma current and inductance as function of plasma resistance, non-inductive current drive sources and boundary loop voltage / PF coil current time derivatives.

2. BACKGROUND

This section outlines the standard Poynting´s and flux balance analysis applied to a tokamak [3] . The mathematical derivation used leads to some intermediate results are used later to derive the internal inductance dynamic equation.

A cylindrical coordinate system is used (r,ϕ,z) and the plasma is assumed to be axis-symmetric around the z-axis. Only the time evolving components (B_r, B_Z) of the *poloidal* magnetic field are considered in the analysis .

The region of integration will be delimited by the region where there is a plasma. This will correspond to a plasma volume G , or a plasma cross section Ω.

The magnetic energy stored in the plasma volume G is obtained from poloidal magnetic field as

$$W = \frac{1}{2\mu}\int_G \left(B_r^2 + B_z^2\right) dv \qquad (1)$$

Where μ is the vacuum magnetic permeability and a volume differential

$$dv = r dr d\phi dz \tag{2}$$

This contains magnetic field created by the plasma current as well as magnetic field created by external conductors.

Using the vector potential with Coulomb gauge

$$\mathbf{A} = \begin{pmatrix} A_r & A_\phi & A_z \end{pmatrix} = \begin{pmatrix} 0 & \psi/2\pi r & 0 \end{pmatrix} \tag{3}$$

where ψ is the flux through an arbitrary circle of radius r centred at the torus symmetry axis, the magnetic field can be obtained from a vector potential, as

$$\mathbf{B} = \nabla \times \mathbf{A} \tag{4}$$

This renders the usual expressions for magnetic field components in a tokamak

$$\begin{aligned} B_r &= -\frac{\partial A_\phi}{\partial z} = -\frac{1}{2\pi r}\frac{\partial \psi}{\partial z} \\ B_z &= \frac{1}{r}\frac{\partial \left(r A_\phi \right)}{\partial r} = \frac{1}{2\pi r}\frac{\partial \psi}{\partial r} \end{aligned} \tag{5}$$

Similarly, the toroidal current density is obtained from magnetic field as

$$\mu \mathbf{j} = \nabla \times \mathbf{B} \tag{6}$$

Using the vector identity

$$B^2 = \nabla \cdot \left(\mathbf{A} \times \mathbf{B} \right) + \mu \mathbf{A} \mathbf{j} \tag{7}$$

the magnetic energy   (1) can then be written as

$$W = \frac{\int_G \mathbf{Aj}dv - \psi_B I}{2} \tag{8}$$

or in terms of flux [11]

$$W = \frac{\int_\Omega \psi\, jdS - \psi_B I}{2} \tag{9}$$

where $dS = drdz$, j is the toroidal current density, ψ_B is the flux at the plasma boundary Ω and I is the total plasma current enclosed by this boundary.

$$I = \int_\Omega jdS \tag{10}$$

Using Lenz´s law, the voltage at any location is obtained from flux as

$$V = -\frac{d\psi}{dt} \tag{11}$$

And in particular, the boundary loop voltage is

$$V_B = -\frac{d\psi_B}{dt} \tag{12}$$

Time derivative of (9) leads to the Poynting´s theorem

$$\frac{dW}{dt} + \int_\Omega jVdS = V_B I \tag{13}$$

To obtain (13) we have used the identity

$$\mu \mathbf{A}\frac{\partial \mathbf{j}}{\partial t} = \mathbf{A}\cdot\left(\nabla\times\frac{\partial \mathbf{B}}{\partial t}\right) = -\nabla\cdot\left(\mathbf{A}\times\frac{\partial \mathbf{B}}{\partial t}\right) + \frac{\partial \mathbf{B}}{\partial t}\cdot\left(\nabla\times\mathbf{A}\right) \tag{14}$$

and an integration over the plasma volume to obtain

$$\int_{\Omega}\psi\frac{\partial j}{\partial t}dS = \int_{G}A\frac{\partial j}{\partial t}dv = \psi_b\frac{dI}{dt} + \frac{dW}{dt} \tag{15}$$

The toroidal current density can be written in terms of ohmic and non inductive current drive components. Define η and $\hat{j}$ as effective plasma resistivity and non-inductive current density in the toroidal direction. Then, ohms law is written as

$$E = \eta\left(j - \hat{j}\right) \tag{16}$$

Where Define plasma resistance as

$$R = \frac{\int_{\Omega}\eta j^2 dS}{I^2} \tag{17}$$

Define non inductive current drive fraction as

$$\frac{\hat{I}}{I} = \frac{\int_{\Omega} j\eta\hat{j}dS}{\int_{\Omega}\eta j^2 dS} \tag{18}$$

And define an ideal non inductive voltage source equivalent

$$\hat{V} = R\hat{I} = \frac{\int_{\Omega} j\eta\hat{j}dS}{I} \tag{19}$$

These definitions lead to the circuit equation

$$\frac{dW}{dt} + V_R I = V_B I \tag{20}$$

The resistive voltage drop can be written in terms of the total plasma current and an equivalent non-inductive current $\hat{I}$ or voltage $\hat{V}$ equivalent source.

$$V_R = R\left(I - \hat{I}\right) = RI - \hat{V} \tag{21}$$

Following electrical engineering standards, the internal inductance is defined from the magnetic energy W stored in the poloidal field in the region enclosed by the plasma boundary

$$L_i = \frac{2W}{I^2} \tag{22}$$

Leading to

$$V_B = V_R + \frac{1}{I}\frac{d}{dt}\left(\frac{1}{2}L_i I^2\right) \tag{23}$$

The inductive voltage is defined as

$$V_{ind} = V_B - V_R = \frac{1}{I}\frac{d}{dt}\left(\frac{1}{2}L_i I^2\right) \tag{24}$$

Time integration of (23) leads to

$$\psi_B = \psi_R + \psi_{ind} \tag{25}$$

Where the inductive and resistive fluxes in (25) are identified from (23) as [3]

$$\psi_R = -\int_0^t V_R dt = -\int_0^t R\left(I - \hat{I}\right) dt \tag{26}$$

$$\psi_{ind} = -\int_0^t V_{ind} dt = -\int_0^t \frac{1}{I}\frac{d}{dt}\left(\frac{1}{2}L_i I^2\right)dt = -L_i I + \frac{1}{2}\int_0^t I\frac{dL_i}{dt}dt \qquad (27)$$

The sign criteria in the above equations differs from the one given in [3]. In our case, is given by Lenz's law (11) and Ohm's law (21) written in cylindrical coordinates. With this sign convention a boundary flux that increases in time will generate a negative boundary loop voltage and a negative plasma current. The applied boundary flux is invested according to (25) in inductive (27) and resistive (26) flux components .

Finally, the flux at the plasma boundary can be written as the sum of the flux due to the plasma internal current density and the flux due to the external PF system [14]

$$\psi_b = L_e I + \sum M_j I_j \qquad (28)$$

where L_e is the plasma external inductance and M_j are the mutual inductances between PF coils and plasma.

The mutual inductance M_j is function of the coil and plasma boundary geometry. It is defined from the line integral of the vector potential A_j due to the coil system j along a field line covering the plasma boundary:

$$M_j = \frac{\int_\Omega A_j dl}{I_j N} \qquad (29)$$

Where N the number of turns of the field line around the machine symmetry axis.

The external inductance is similarly defined from the line integral of the vector potential A due to the plasma current distribution along a field line covering the plasma boundary.

$$L_e = \frac{\int_\Omega A dl}{IN} \qquad (30)$$

The external inductance is mainly a function of the plasma boundary geometry, with a weak dependence on the flux gradient at the plasma boundary [15].

Combining (25), (28),(27) we obtain

$$\left(L_e + L_i\right) I + \sum M_j I_j = \psi_R + \frac{1}{2}\int_0^t I \frac{dL_i}{dt} dt \tag{31}$$

Which is a transformer equation in which the plasma secondary has a equivalent plasma inductance

$$L_p = L_e + L_i \tag{32}$$

This transformer equation is more easily recognised if we fix constant the plasma inductance and take time derivatives

$$-\sum M_j \frac{dI_j}{dt} = R\left(I - \hat{I}\right) + L_P \frac{dI}{dt} \tag{33}$$

The change of flux produced by external coils generates a voltage that compensates the resistive drop and builds up the plasma current.

3. STATE SPACE MODEL

We are after a state space description of the plasma with current I and internal inductance L_i as output variables and plasma resistance, non inductive current drive, and boundary loop voltage as inputs.

We start by introducing the current density weighted flux average

$$\psi_C = \frac{\int_\Omega \psi \, j dS}{I} \tag{34}$$

This flux depends on the particular plasma flux and current profile shapes, or equilibrium. We will refer to the *equilibrium flux surface* as the flux surface corresponding to ψ_C.

Using (9),(34) the poloidal field magnetic energy can then be written as

$$W = \frac{(\psi_C - \psi_B) I}{2} \tag{35}$$

And using (22)

$$L_i I = (\psi_C - \psi_B) \tag{36}$$

This implies $\psi_C < \psi_B$ for negative plasma current.

Time derivative of (34) leads to

$$\psi_C \frac{dI}{dt} - \int_\Omega \psi \frac{\partial j}{\partial t} dS = (V_C - V_R) I \tag{37}$$

Where the voltage at the equilibrium flux surface is

$$V_C = -\frac{d\psi_C}{dt} \tag{38}$$

And using (15), (20) and (23) we finally obtain

$$I \frac{dL_i}{dt} = 2(V_R - V_C) \tag{39}$$

$$L_i \frac{dI}{dt} = V_B + V_C - 2V_R \tag{40}$$

These are exact equations not found in previous literature. They govern plasma current and internal inductance dynamics as function of the applied boundary voltage, plasma resistive voltage and voltage at the equilibrium flux surface.

Internal inductance reaches steady state conditions when $V_C = V_R$. The steady state solution for the full set of equations corresponds with $V_C = V_R = V_B$, or a constant loop voltage profile across the plasma.

To complete the model we must find a third equation for the equilibrium voltage V_C as function of the applied boundary voltage and resistive drop changes. Flux diffusion evolves to achieve a constant loop voltage profile that equals the boundary loop voltage. A first order approximation for this process is obtained by writing

$$\frac{d\left(V_C - V_B\right)}{dt} \cong -\frac{\left(V_C - V_B\right)}{\tau} + \frac{k}{\tau}\left(V_R - V_B\right) \tag{41}$$

Where k, τ are a gain and a time constant. The validity of (41) will be checked in a later section. Regardless of the approximation used, the inductance evolves as result of the competition between resistive drop voltage and voltage at the equilibrium flux surface, according to (39).

The approximation (41) can be incorporated in the state space model by making the change of variables

$$V = V_C - V_B \tag{42}$$

$$I \frac{dL_i}{dt} = 2\left(V_R - V_B\right) - 2V \tag{43}$$

$$L_i \frac{dI}{dt} = 2\left(V_B - V_R\right) + V \tag{44}$$

$$\frac{dV}{dt} \cong -\frac{V}{\tau} + \frac{k}{\tau}\left(V_R - V_B\right) \tag{45}$$

The equations (43),(44), (45) define a 3[th] order state space system as function of the inductive voltage $V_B - V_R$. Making use of (21), a closed set of equations as function of boundary voltage, plasma resistance and current drive is obtained. The model parameters $\{k, \tau\}$ can then be found by running an optimization algorithm that search in the parameter space to find the best match to experimental data. This will be shown in a later section.

4. ALTERNATIVE STATE SPACE MODEL FORMULATION

The model can be written in an alternative form if we integrate (41) from an initial time $t = t_0$

$$V_C - V_B \cong \frac{(\psi_C - \psi_B)}{\tau} - \frac{k}{\tau}(\psi_R - \psi_B) + C \tag{46}$$

Where the integration constant C is

$$C = \left(\left(\psi_C(t_0) - \psi_B(t_0) \right) + k\left(\psi_R(t_0) - \psi_B(t_0) \right) \right) \Big/ \tau - \left(V_C(t_0) - V_B(t_0) \right) \tag{47}$$

Relative to the initial conditions we can write

$$V_C - V_B \cong \frac{(\psi_R - \psi_B)}{\tau} \left(\frac{(\psi_C - \psi_B)}{(\psi_R - \psi_B)} - k \right) \tag{48}$$

Which is just the integral formulation of the derivative approximation (41)

To obtain the model in compact form, we introduce the state space vector

$$x = (x_1, x_2, x_3)^T \tag{49}$$

with

$$x_3 = \frac{(\psi_C - \psi_B)}{(\psi_R - \psi_B)} \tag{50}$$

$$x_2 = x_3 I \tag{51}$$

$$x_1 = \frac{L_i}{x_3^2} \tag{52}$$

With these new variables the magnetic energy is

$$W_m = \frac{L_i I^2}{2} = \frac{x_1 x_2^2}{2} \tag{53}$$

And the inductive flux is

$$\psi_{ind} = -\left(\psi_R - \psi_B\right) = -x_1 x_2 \tag{54}$$

Differentiation of the states using (39), (40), (11) and recursively writing the result as function of the states leads after some algebra to the following state equations

$$\frac{dx_1}{dt} = \frac{2\left(x_3 - 1\right)}{x_2 x_3}\left(V_b - \frac{Rx_2}{x_3} + R\hat{I}\right) \tag{55}$$

$$\frac{dx_2}{dt} = \frac{\left(2 - x_3\right)}{x_1 x_3}\left(V_b - \frac{Rx_2}{x_3} + R\hat{I}\right) \tag{56}$$

$$\frac{dx_3}{dt} \cong \frac{\left(k - x_3\right)}{\tau} - \frac{x_3}{x_1 x_2}\left(V_b - \frac{Rx_2}{x_3} + R\hat{I}\right) \tag{57}$$

The first two equations (55), (56) are exact. The last equation (57) is obtained by writing the approximation (48) as function of the state variables

$$V_C = \frac{(x_3 - k) x_1 x_2}{\tau} + V_B \tag{58}$$

and then substituting the result in the exact differential equation for the state x_3.

$$\frac{dx_3}{dt} = \frac{\left(1 - x_3\right)}{x_1 x_2}\left(V_b - \frac{Rx_2}{x_3} + R\hat{I}\right) + \frac{1}{x_1 x_2}\left(\frac{Rx_2}{x_3} - R\hat{I} - V_c\right) \tag{59}$$

The system of equations (55), (56) and (57) responds to an inductive voltage input encompassing external boundary voltage stimuli, plasma resistance changes and non inductive current drive sources.

$$u_1\left(V_b, R, \hat{I}, x\right) = V_b - \frac{Rx_2}{x_3} + R\hat{I} \tag{60}$$

The state space equations (55), (56) and (57) can be integrated in time starting from some given initial conditions for the states, and together with the output equations

$$y = \left(y_1, y_2\right)^T = \left(L_i, I\right)^T \tag{61}$$

$$L_i = x_1 x_3^2 \tag{62}$$

$$I = \frac{x_2}{x_3} \tag{63}$$

constitute an alternative formulation that is equivalent to the one given by (43), (44), (45). Both models produce identical results.The difference is that the approximation for flux diffusion is given in differential form in one case, and in integral form in the other.

Following the standards in non linear state space formulation for non-linear systems [16], the model can be written in a more compact form as

$$\begin{aligned} \frac{dx}{dt} &= f_1(x) + g_1(x)\, u_1\left(V_b, R, \hat{I}, x\right) \\ y &= h(x) \end{aligned} \tag{64}$$

With $$f_1(x) = \left(0, 0, \frac{\left(k - x_3\right)}{\tau} \right)^T \qquad 65)$$

$$g_1(x) = \left(\frac{2\left(x_3 - 1\right)}{x_2 x_3} \quad \frac{\left(2 - x_3\right)}{x_1 x_3} \quad -\frac{x_3}{x_1 x_2} \right)^T \tag{66}$$

$$h(x) = \left(x_1 x_3^2, \frac{x_2}{x_3} \right) \tag{67}$$

This model has the inductance and plasma current as output variables by choice. Using the state space formalism, any function of the states and inputs can be made available as an output equation. For instance magnetic energy (53), (54) voltage at the equilibrium flux surface (58)etc, can be made available by writing the corresponding functions of the states and inputs as model outputs.

Also, augmenting the model with new states such as

$$\frac{dx_4}{dt} = -V_b \tag{68}$$

The boundary and resistive fluxes can be also be made available as output equations

$$\begin{aligned} \psi_B &= x_4 \\ \psi_R &= x_1 x_2 + x_4 \end{aligned} \tag{69}$$

and from here, the Ejima coefficient [3],[5] can also be obtained as an output equation

$$C_E = \frac{\psi_R}{\mu_0 r_0 I} = \frac{\left(x_1 x_2 + x_4 \right) x_3}{\mu_0 r_0 x_2} \tag{70}$$

where r_0 is the magnetic axis coordinate.

Also, an output equation for the dimensionless internal inductance [17] could be made available as

$$l_i = \frac{4W}{\mu_0 r_0 I^2} = \frac{2L_i}{\mu_0 r_0} = \frac{2x_1 x_3^2}{\mu_0 r_0} \tag{71}$$

This last normalization is the standard used for the ITER design [6].

5. STATE SPACE MODEL AS FUNCTION OF POLOIDAL FIELD CURRENTS

Finally, we have to write the model as function of the PF coil currents surrounding the plasma. For constant M_j, L_e (fixed plasma geometry), Lenz´s law applied to the boundary flux balance (28) leads to

$$V_B = -L_e \frac{dI}{dt} - M_j \frac{dI_j}{dt} \tag{72}$$

Which combined with (40) leads to

$$V_B = \left(\frac{-L_i}{(L_i + L_e)} \right) M_j \frac{dI_j}{dt} - \frac{L_e}{(L_i + L_e)} (V_C - 2V_R) \tag{73}$$

And using (21) (58) (62) (63) the inductive voltage (60)can be written as

$$\left(V_b - \frac{Rx_2}{x_3} + R\hat{I} \right) = -\frac{L_e}{\left(x_1 x_3^2 + 2L_e\right)} \left(\frac{(x_3 - k)x_1 x_2}{\tau} \right) + \frac{x_1 x_3^2}{\left(x_1 x_3^2 + 2L_e\right)} \left(-\sum_{j=1}^{N} M_j \frac{dI_j}{dt} - \frac{Rx_2}{x_3} + R\hat{I} \right) \tag{74}$$

The validity of this expression is conditioned to the validity of the approximation (58). The inductive voltage (74)can then be incorporated into the state equations (55), (56) and (57) , and the state space model can then finally be written in compact form as

$$\begin{aligned} \frac{dx}{dt} &= f_2(x) + g_2(x) u_2\left(V_b, R, \hat{I}, x\right) \\ y &= h(x) \end{aligned} \tag{75}$$

With $h(x)$ given by (67) , and

$$u_2\left(I_j, R, \hat{I}, x\right) = -\sum_{j=1}^{N} M_j \frac{dI_j}{dt} - \frac{Rx_2}{x_3} + R\hat{I} \tag{76}$$

$$g_2(x) = \frac{x_1 x_3^2}{\left(x_1 x_3^2 + 2L_e\right)} g_1(x) \tag{77}$$

$$f_2(x) = -\frac{L_e}{\left(x_1 x_3^2 + 2L_e\right)}\left(\frac{(x_3 - k)x_1 x_2}{\tau}\right) g_1(x) + f_1(x) \tag{78}$$

Where the new input to the state space equations is now a function of the PF coil drive, plasma resistance and non inductive current drive. Same procedure can be applied to the case where external and mutual inductances are function of time, resulting in an additional input to (76)

$$u_2\left(I_j, R, \hat{I}, x\right) = -\sum_{j=1}^{N} M_j \frac{dI_j}{dt} - \frac{Rx_2}{x_3} + R\hat{I} - \sum_{j=1}^{N} I_j \frac{dM_j}{dt} - I\frac{dL_e}{dt} \tag{79}$$

6. STATE SPACE MODEL VALIDATION

To validate the state space model we use the actual readings of real time diagnostics at the JET tokamak. Plasma resistance and boundary voltage are inputs the state space model given by equations (55), (56), (57) with an initial guess for the initial conditions and the adjustable parameters $\{k, \tau\}$. The current and inductance outputs of the state space model are then compared with the actual JET data and an optimization algorithm is used to search on the initial conditions and parameter space to find the best match in the Akaike´s final prediction error sense [18]. The figures below show simulation results for an optimized cases with fixed $k \cong 0.98$ and $\tau \cong 1.25$, for two discharges with step up/down on plasma current in the flat top and negligible current drive. The first order approximation for the flux diffusion process along with the non linear relationships in the state space model are sufficient to reproduce the experimental data with reasonable accuracy. Of course running the optimization using data segmentation for the three distinct phases (ramp-up, flat top and ramp-down) can increase the accuracy of the simulations providing different sets of parameters for each segment. But the interesting point here is that a first order approximation with two parameters $\{k, \tau\}$ can reproduce most of the experimental data with reasonable accuracy.

7. RELATIONSHIP BETWEEN INDUCTANCE AND PLASMA CURRENT RAMP-RATE

Taking the ratio between (55) and (56)

$$\frac{1}{x_1}\frac{dx_1}{dt} = \frac{2\left(x_3 - 1\right)}{\left(2 - x_3\right)}\frac{1}{x_2}\frac{dx_2}{dt} \tag{80}$$

And using (52), (51) and (50) we arrive to

$$\frac{dL_i}{dt}=\frac{2\left(x_3-1\right)}{\left(2-x_3\right)}\frac{L_i}{I}\frac{dI}{dt}+\frac{2L_i}{x_3\left(2-x_3\right)}\frac{dx_3}{dt} \tag{81}$$

A common misunderstanding or language abuse is to state that the internal inductance changes are produced by plasma current ramp rates. Equation (81) quantifies a correlation between plasma current ramp rates and internal inductance changes, but it does not imply a cause effect relationship between current ramp rates and inductance changes. Both plasma current and inductance have a common cause, which is the applied inductive voltage to the plasma. Because they have a common cause, they exhibit a correlation. But the internal inductance evolves depending of the competition between resistive drop voltage and voltage at the equilibrium flux surface, according to (39). The existing correlation , however, has successfully been exploited to control the internal inductance using the plasma current ramp rate as a virtual actuator [6].

A more direct option is to use directly the transformer coil as the actuator. In any case, the state space models presented can be used as the keystone for the design [19].

CONCLUSIONS

Using a first order approximation for flux diffusion dynamics together with energy conservation and flux balance theorems, a non linear model for plasma current and inductance time evolution as function of plasma resistance, non-inductive current drive and boundary loop voltage / PF coil current time derivatives has been obtained. The model is expressed in state space form, the preferred choice for the design of control systems using modern control systems theory. The choice of system states allow many interesting physical quantities such as plasma current, inductance, magnetic energy, resistive and inductive fluxes etc be made available as output equations. The validity of this model has been checked using experimental data from JET showing an excellent agreement.

Contrary to what is commonly believed, plasma current ramp rates are not the cause of internal inductance changes, although both are strongly correlated under some circumstances. A mathematical expression for this correlation has been derived from the state space model.

ACKNOWLEDGMENT

The authors are very grateful to UPV/EHU and the Science and Innovation Council MICINN for its support through research projects GIU07/08, DPI2006-01677 and ENE2009-07200 respectively. They are also grateful to the Basque Government for its partial support through the research projects S-PE07UN04, S-PE08UN15 and S-PE09UN14.

This work, supported by the European Communities under the contract of Association between EURATOM and Ciemat, was carried out within the framework of the European Fusion Development Agreement. The views and opinions expressed herein do not necessarily reflect those of the European Commission.

REFERENCES

[1] R. Nishi, A. Takaoka and K. Ura. Frequency Dependence of Inductance Due to Slow Flux Penetration into Magnetic Circuit of Lens. Journal of Electron Microscopy 42(1): 31-34 (1993)

[2] O.M.O Gatous and J. Pissolato. Frequency-dependent skin-effect formulation for resistance and internal inductance of a solid cylindrical conductor. IEE Proc., Microw. Antennas Propag. (2004) Vol.151, Issue 3, p.212–216.

[3] Ejima et al. . Volt second analysis of D-III discharges. Nuclear Fusion Vol. 22. No 10 (1982).

[4] W.A.Houlberg . Volt second consumption in tokamaks with sawtooth activity. Nuclear Fusion Vol. 27. No 6 (1987).

[5] S.C. Jardin. Poloidal Flux Linkage requirements for the international thermonuclear experimental reactor. Nuclear Fusion Vol.34, No 8 (1994)

[6] G.L. Jackson, T.A. Casper, T.C. Luce, D.A. Humphreys, J.R. Ferron, A.W. Hyatt, E.A. Lazarus, R.A. Moyer, T.W. Petrie, D.L. Rudakov and W.P. West. ITER startup studies in the DIII-D tokamak. Nucl. Fusion 48 No 12 . Dec. 2008.

[7] M. Ferrara, I.H. Hutchinson and S.M. Wolfe. Plasma Inductance and stability metrics on Alcator C-mod. Nucl. Fusion 48 (2008) 065002

[8] J.Leuer, J. Lister, L.L. LoDestro, W.H. Meyer,L.D. Pearlstein, A. Portone, F. Sartori, M.L. Walker,A.S.Welander and S.M.Wolfe. “Experimental vertical stability studies for ITER performance and design guidance” Nucl. Fusion 49 (2009) 115003

[9] C.E. Kessel, D. Campbell, Y. Gribov, G. Saibene, G. Ambrosino, R.V. Budny, T. Casper, M. Cavinato, H. Fujieda, R. Hawryluk, L.D. Horton, A. Kavin, R. Kharyrutdinov, F. Koechl, J. Leuer, A. Loarte, P.J. Lomas, T. Luce, V. Lukash, M. Mattei, I. Nunes, V. Parail1, A. Polevoi, A. Portone, R. Sartori, A.C.C. Sips, P.R. Thomas, A. Welander and J. Wesley. Development of ITER 15MA ELMy H-mode inductive scenario. Nucl. Fusion 49 (2009) 085034

[10] Y. Nakamura, K. Tobita, A. Fukuyama, N. Takei, Y. Takase, T. Ozeki1 and S.C. Jardin. *simulation study on inductive ITB control in reversed shear tokamak discharges*. Nucl. Fusion 46 (2006) S645–S651

[11] R. Albanese and F. Villone. *The linearized CREATE-L plasma response model for the control of current, position and shape in tokamaks*. Nuclear Fusion, Vol. 38, No. 5 (1998)

[12] R.J. Hawryluk, D.J. Campbell, G. Janeschitz, P.R. Thomas, R. Albanese,R. Ambrosino, C. Bachmann, L. Baylor, M. Becoulet, I. Benfatto, J. Biale,A. Boozer, A. Brooks, R. Budny, T. Casper, M. Cavinato, J.-J. Cordier,V. Chuyanov, E. Doyle, T. Evans, G. Federici, M. Fenstermacher, H. Fujieda,K. G'al, A. Garofalo, L. Garzotti, D. Gates, Y. Gribov, P. Heitzenroeder,T.C. Hender, N. Holtkamp, D. Humphreys, I. Hutchinson, K. Ioki, J. Johner,G. Johnson, Y. Kamada, A. Kavin, C. Kessel, R. Khayrutdinov, G. Kramer,A. Kukushkin, K. Lackner, I. Landman, P. Lang, Y. Liang, J. Linke, B. Lipschultz, A. Loarte, G.D. Loesser, C. Lowry, T. Luce, V. Lukash,S. Maruyama, M. Mattei, J. Menard, M. Merola, A. Mineev, N. Mitchell,E. Nardon, R. Nazikian, B. Nelson, C. Neumeyer, J.-K. Park, R. Pearce,R.A. Pitts, A. Polevoi, A. Portone, M. Okabayashi, P.H. Rebut, V. Riccardo,J. Roth, S. Sabbagh, G. Saibene, G. Sannazzaro, M. Schaffer M. Shimada, A. Sen, A. Sips, C.H. Skinner, P. Snyder, R. Stambaugh, E. Strait,M. Sugihara, E. Tsitrone, J. Urano, M. Valovic, M. Wade, J. Wesley,R. White, D.G. Whyte, S. Wu, M. Wykes and L. Zakharov "Principal physics developments evaluated in the ITER design review". Nucl. Fusion 49 (2009) 065012

[13] L. Ljung. System Identification: Theory for the user. PTR Prentice Hall, 1987. ISBN 0-13-881640-9

[14] S.P. Hirshman and G.P. Neilson. External Inductance of an axisymmetric plasma. Phys.Fluids 29 (3) March 1986.

[15] G.O. Ludwig and M.C.R. Andrade. External inductance of large ultralow aspect ratio tokamak plasmas. Physics of plasmas 5 (6). June 1998.

[16] J.J.E. Slotine, Weiping Li. Applied Nonlinear Control. Prentice Hall., 1991. ch.6. ISBN 0-13-040890-5

[17] Shafranov. Reviews of plasma physics. Vol 2. (Leontovich, M.A., Ed.), Consultants Bureau, New York (1966) 103

[18] Akaike, Hirotugu (1974). *A new look at the statistical model identification*. IEEE Transactions on Automatic Control 19 (6): 716–723.

[19] J.A. Romero, C. D. Challis, R. Felton, E. Jachmich, E. Joffrin, D. Lopez-Bruna , F. Piccolo, P. Sartori, A.C.C. Sips, P. de Vries, L. Zabeo and JET-EFDA contributors. "Tokamak plasma inductance control at JET". 36th EPS Conference on Plasma Phys, Sofia, June 29 - July 3, 2009.

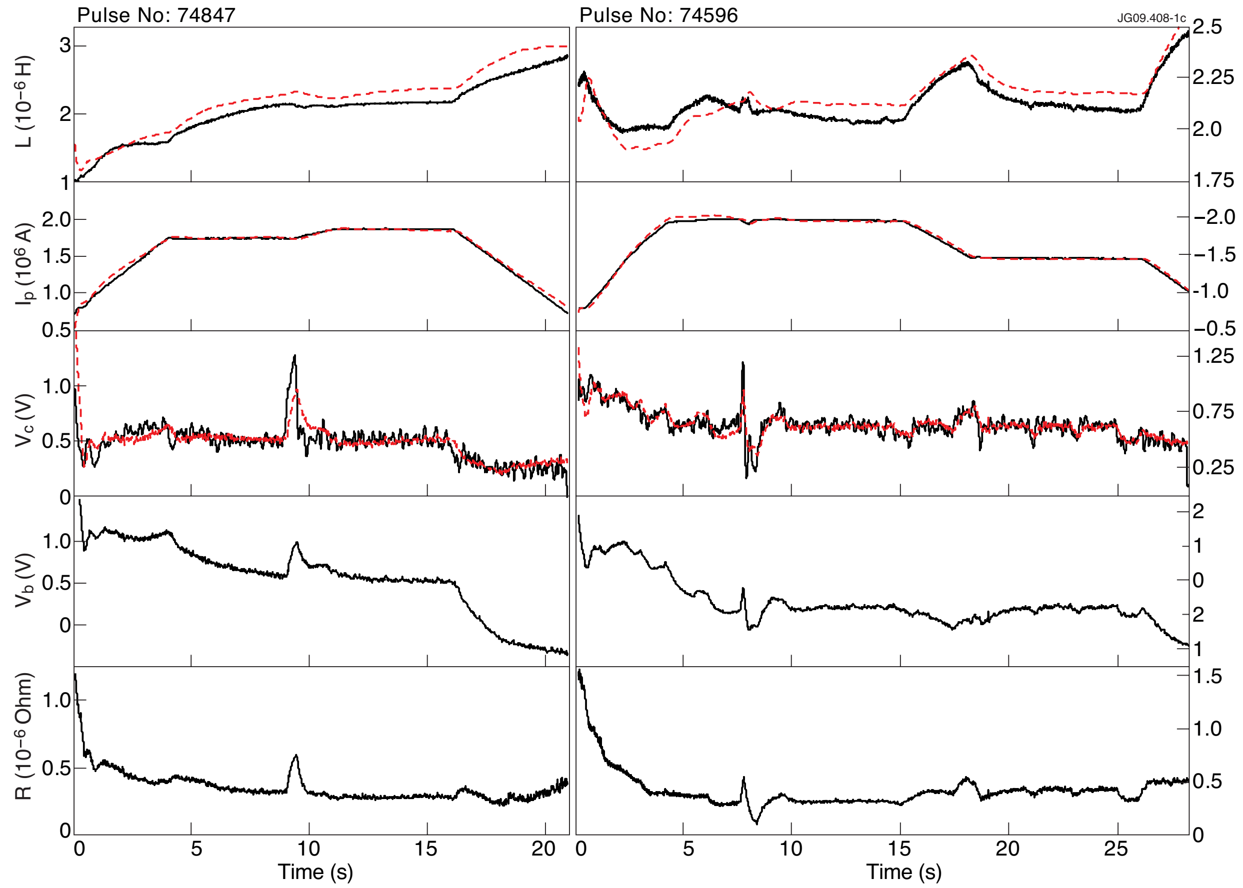

Figure 1: Comparison between experimental readings (black) and state space model outputs (red). In top-down order are shown the plasma internal inductance, plasma current, voltage V_C at the equilibrium flux surface ψ_C, boundary voltage and plasma resistance.